Published in final edited form as:
Heart Rhythm. 2011 July ; 8(7): 1024–1032. doi:10.1016/j.hrthm.2011.02.021.

Transient Outward Current (I_{to}) Gain-of-Function Mutations in the *KCND3*-Encoded Kv4.3 Potassium Channel and Brugada Syndrome

John R. Giudicessi, BA[1,2,*], **Dan Ye, MD**[1,*], **David J. Tester, BS**[1], **Lia Crotti, MD, PhD**[3,4,5], **Alessandra Mugione, PhD**[5], **Vladislav V. Nesterenko, PhD**[8], **Richard M. Albertson, BS**[1], **Charles Antzelevitch, PhD**[8], **Peter J. Schwartz, MD**[3,4,5,6,7], and **Michael J. Ackerman, MD, PhD**[1]

[1]Departments of Medicine (Division of Cardiovascular Diseases), Pediatrics (Division of Pediatric Cardiology), and Molecular Pharmacology & Experimental Therapeutics, Windland Smith Rice Sudden Death Genomics Laboratory, Mayo Clinic, Rochester, MN

[2]Mayo Medical School, Mayo Clinic, Rochester, MN

[3]Department of Lung, Blood, and Heart, University of Pavia, Pavia Italy

[4]Department of Cardiology, Fondazione IRCCS Policlinico San Matteo, Pavia Italy

[5]Laboratory of Cardiovascular Genetics, IRCCS Istituto Auxlogico, Milan, Italy

[6]Cardiovascular Genetics Laboratory, Hatter Institute for Cardiovascular Research, Department of Medicine, University of Cape Town, South Africa

[7]Chair of Sudden Death, Department of Family and Community Medicine, College of Medicine, King Saud University, Riyadh, Saudi Arabia

[8]Masonic Medical Research Laboratory, Utica, NY

Abstract

Background—Brugada syndrome (BrS) is a sudden death predisposing genetic condition characterized electrocardiographically by ST-segment elevation in the leads V_1-V_3. Given the prominent role of the transient outward current (I_{to}) in BrS pathogenesis, we hypothesized that rare gain-of-function mutations in *KCND3* may serve as a pathogenic substrate for BrS.

Methods—Comprehensive mutational analysis of *KCND3*-encoded Kv4.3 (I_{to}) was conducted using PCR, DHPLC, and direct sequencing of DNA derived from 86 unrelated BrS1-8 genotype negative BrS patients. DNA from 780 healthy individuals was examined to assess allelic frequency for non-synonymous variants. Putative BrS-associated Kv4.3 mutations were

Reprints and correspondence: Michael J. Ackerman, M.D., Ph.D., Mayo Clinic Windland Smith Rice Sudden Death Genomics Laboratory, Guggenheim 501, Mayo Clinic, Rochester, MN 55905, 507-284-0101 (phone), 507-284-3757 (fax), ackerman.michael@mayo.edu.
*J.R.G. and D.Y. are co-equal first authors.

Conflict of Interest

MJA is a consultant for Transgenomic/FAMILION. Intellectual property derived from MJA's research program resulted in license agreements in 2004 between Mayo Clinic Health Solutions (formerly Mayo Medical Ventures) and PGxHealth (recently acquired by Transgenomic).

engineered and co-expressed with wild-type KChIP2 in HEK293 cells. Wild-type and mutant I_{to} ion currents were recorded using whole cell patch clamp.

Results—Two BrS1-8 genotype-negative cases possessed novel Kv4.3 missense mutations. Both Kv4.3-L450F and Kv4.3-G600R were absent in 1560 reference alleles and involved residues highly conserved across species. Both Kv4.3-L450F and Kv4.3-G600R demonstrated a gain-of-function phenotype, increasing peak I_{to} current density by 146.2% (n=15, p<0.05) and 50.4% (n=15, p<0.05) respectively. Simulations employing a Luo-Rudy II AP model demonstrated the stable loss of the AP dome as a result of the increased I_{to} maximal conductance associated with the heterozygous expression of either L450F or G600R.

Conclusions—These findings provide the first molecular and functional evidence implicating novel *KCND3* gain-of-function mutations in the pathogenesis and phenotypic expression of BrS, with the potential for a lethal arrhythmia being precipitated by a genetically enhanced I_{to} current gradient within the right ventricle were *KCND3* expression is the highest.

Keywords

Brugada syndrome; genetic diseases; ion channels, I_{to} current; J wave syndromes; Kv4.3 channels; sudden cardiac death

INTRODUCTION

Sudden cardiac death (SCD) accounts for approximately 300,000 deaths in the United States annually.[1] While structural heart disease represents the primary etiology of SCD in the general population, it is estimated that as many as one-third of young cases and 5–10% of all SCD occur within individuals with no detectable structural abnormalities upon postmortem investigation.[2, 3] Tragically, thousands of individuals under the age of 40 with otherwise structurally normal hearts die suddenly each year representing a loss of life-years that rivals ischemic-related heart disease.[2,4] Cardiac channelopathies such as catecholaminergic polymorphic ventricular tachycardia, long QT syndrome (LQTS), and Brugada syndrome (BrS) which arise from heritable defects in cardiac ion channel function represent the most common identifiable causes underlying autopsy negative sudden unexplained death.[5]

BrS affects as many as 1 in 2500 individuals and is characterized electrocardiographically by dynamic coved-type ST-segment elevation in the right precordial leads in the absence of ischemia, structural heart disease, and pharmacologic agents known to induce a BrS-like ECG pattern.[6, 7] Affected individuals are typically males in the 4th decade of life with a high incidence of syncope and sudden death secondary to ventricular arrhythmias that often develop during times of increased vagal activity such as sleep or rest. Due to the variable penetrance and expressivity of this autosomal-dominant disorder, the clinical course of BrS assumes a spectrum that includes lifelong asymptomatic individuals as well as those who die suddenly in early life, including infancy.[8] It is estimated that BrS accounts for nearly 5% of all sudden deaths and up to 20% of sudden deaths in individuals with otherwise structurally normal hearts.[7]

Since its seminal description as a clinical entity in 1992, BrS has been linked to mutations in genes that perturb cardiac sodium (I_{Na}), calcium ($I_{Ca.L}$), or potassium (I_{to} and $I_{K\text{-}ATP}$) channel function. At the cellular and ionic level, insufficient sodium (I_{Na}) or calcium (I_{Ca}) inward depolarizing current coupled with a right ventricular transmural gradient (epicardium > endocardium) involving the transient outward repolarizing current (I_{to}) conducted by the *KCND3*-encoded Kv4.3 α-subunit is hypothesized to result in an outward shift in current, heterogenous loss of the action potential dome, ST segment elevation on ECG, local re-excitation via phase II reentry, and the initiation of polymorphic ventricular tachycardia or

ventricular fibrillation.[9] The recent identification of 1) a BrS-associated loss-of-function missense mutation in the negative modulating *KCNE3*-encoded MiRP2 Kv4.3 β-subunit[10] that significantly increases I_{to} current and 2) a J wave syndrome-associated pleiotropic gain-of-function missense mutation in the *KCNJ8*-encoded Kir6.1 α-subunit of the ATP-sensitive potassium ($I_{K\text{-}ATP}$) channel[11] have strengthened the hypothesis that a gain-of-function in outward potassium currents (I_{to} and $I_{K\text{-}ATP}$) active during early repolarization can contribute to the pathogenesis of BrS and other disorders of early repolarization. Despite the major advances in the understanding of the cellular, ionic, and genetic basis of BrS, an estimated 60% to 70% of BrS cases remain genetically elusive.

Even though no mutations in the *KCND3*-encoded Kv4.3 channel have been identified to date, we hypothesized that rare gain-of-function mutations in *KCND3* may confer risk for lethal atrial or ventricular arrhythmias and thus may serve as the pathogenic substrate for some genetically elusive cases of BrS. In this study, we sought to determine the spectrum and prevalence of *KCND3* mutations in a cohort of 86 BrS patients previously screened for mutations in BrS1-BrS8 with spontaneous or flecainide-induced ST-segment elevation in the right precordial leads in the absence of any structural or ischemic heart disease by echocardiogram and coronary angiogram.

METHODS

Study Population

The study population consisted of 86 unrelated patients diagnosed with BrS on established clinical criteria who were referred to the Windland Smith Rice Sudden Death Genomics Laboratory at Mayo Clinic, Rochester, Minnesota or the Molecular Cardiology Laboratory, Fondazione IRCCS Policlinico San Matteo, Pavia, Italy for laboratory based genetic testing. All BrS cases included in this study were screened previously for mutations in the 8 known BrS-susceptibility genes (*SCN5A, GPD1L, CACNA1C, CACNB2, SCN1B, KCNE3, SCN3B,* and *KCNJ8*).

This study was approved by both the Mayo Foundation Institutional Review Board and the Medical Ethical Committee of Fondazione IRCCS Policlinico San Matteo. Informed consent was obtained for all patients.

Control Population

DNA from a cohort of 780 (680 Caucasian and 100 African American) ostensibly healthy individuals was obtained from the Coriel Cell Repository and the European Collection of Cell Cultures. These samples were used to assess allelic frequency for all identified non-synonymous variants and to independently determine the rate of background genetic variation within *KCND3* among healthy blood donors.

Mutational Analysis

Genomic DNA was extracted from peripheral blood lymphocytes using Purgene DNA extraction kits (Gentra Systems Inc., Minneapolis, MN). Comprehensive mutational analysis of *KCND3* was accomplished in cases and controls using polymerase chain reaction (PCR), denaturing high-performance liquid chromatography (DHLPC), and direct DNA sequencing as previously described.[12] The flanking primers used to amplify *KCND3* were designed using the Primer3 web-based interface.[13] Primer sequences, PCR conditions, and DHPLC conditions are available upon request.

KCND3 and *KCNIP2* Mammalian Expression Vectors and Mutagenesis

Wild-type human *KCND3* cDNA was provided by Charles Antzelevitch. The wild-type human *KCNIP2* cardiac isoform cDNA was synthesized as a custom minigene contained in the pIDTSMART vector backbone (Integrated DNA Technologies, Coralville, IA). Wild-type *KCND3* cDNA was subcloned into pIRES2-EGFP (Clontech, Mountain View, CA) to produce pIRES2-*KCND3*^{WT}-EGFP and wild-type *KCNIP2* cDNA was subcloned into pIRES2-dsRed2 (Clontech, Mountain View, CA) to produce pIRES2-*KCNIP2*^{WT}-dsRed2. The L450F and G600R mutations were engineered into pIRES2-*KCND3*^{WT}-EGFP using the Quikchange XL Site-Directed Mutagenesis Kit (Stratagene, La Jolla, CA). DNA sequencing was used to confirm the integrity of all vectors.

HEK293 Cell Culture and Transfection

HEK293 cells were cultured in minimum essential medium supplemented with 1% nonessential amino acid solution, 10% horse serum, 1% sodium pyruvate solution, and 1.4% penicillin/streptomycin solution. All cells were plated in T25 flasks and stored in a 5% CO_2 incubator at 37°C for 24 hours. Heterologous expression of Kv4.3 and KChIP2 was accomplished by co-transfecting 0.5 μg of pIRES2-*KCND3*^{WT}-EGFP, pIRES2-*KCND3*^{L450F}-EGFP or pIRES2-*KCND3*^{G600R}-EGFP with 1.5 μg pIRES2-*KCNIP2*^{WT}-dsRed2 using 5 μl of Lipofectamine transfection reagent (Invitrogen, Carlsbad, CA) in Gibco® OPTI-MEM media (Invitrogen, Carlsbad, CA). Cells exhibiting both green fluorescence (excitation 488 nm, emission 507 nm) and red fluorescence (excitation 558 nm, emission 583 nm) at 24 hours post-transfection were selected for electrophysiological experiments.

Electrophysiological Measurements and Data Analysis

Standard whole cell patch clamp technique was used to measure Kv4.3-WT, Kv4.3-L450F, or Kv4.3-G600R plus KChIP2-WT currents at room temperature (22–24°C) with the use of an Axopatch 200B amplifier, Digidata 1440A and pClamp version 10.2 software (Axon Instruments, Foster City, CA). The extracellular (bath) solution contained (mmol/L): 140 NaCl, 4 KCl, 2 $CaCl_2$, 1 $MgCl_2$, and 10 HEPES, pH adjusted to 7.4 with NaOH. The pipette solution contained (mmol/L): 110 KCl, 31 KOH, 10 EDTA, 5.17 $CaCl_2$, 1.42 $MgCl_2$, 4 MgATP and 10 HEPES, pH adjusted to 7.2 with KOH following established protocols.[10, 14] Microelectrodes were pulled on a P-97 puller (Sutter Instruments, Novato, CA) and fire polished to a final resistance of 2–3 MΩ. Series resistance was compensated by 80–85%. Currents were filtered at 5 kHz and digitized at 10 kHz. The voltage-dependence of activation, inactivation, and recovery from inactivation were determined using voltage-clamp protocols described in the figure legend. Data was analyzed using Clampfit (Axon Instruments), Excel (Microsoft, Redmond, WA), and fitted with Origin 8 (OriginLab Corporation, Northampton, MA).

Voltage-dependent inactivation curve was fitted with a Boltzmann function: $I/I_{max} = \{1+\exp[(V-V_{1/2})/k]\}^{-1}$, where $V_{1/2}$ and k are the half-maximal voltage of inactivation and the slope factor respectively. Recovery from inactivation was fitted with a one-exponential function: $y=y_0+[A_1 \exp(-x/\tau_1)]$ where A_1 indicates the fractions of recovery from inactivation, τ_1 indicates the time constant for recovery from inactivation. Inactivation time constants for each voltage step were determined by fitting a monoexponential function to current decay. Total charge as a function of voltage obtained by measuring the area under curve during the first 50 ms of each voltage step.

Simulated Ventricular Epicardial Action Potentials

Right ventricular (RV) and left ventricular (LV) epicardial action potentials were simulated using a Luo-Rudy II multi-cellular 1-dimensional fiber AP model, modified to include the I_{to} current, as previously published.[15, 16] The incorporation of I_{to} in the Luo-Rudy II AP model requires decreasing maximal conductance of I_{CaL} by 20% to compensate for the significant increase of I_{CaL} during the notch of the action potential. The maximal conductance of RV I_{to} was set to 1.3 mS/μF for wild-type, 2.32 mS/μF for L450F, and 1.56 mS/μF for G600R in accordance with experimentally derived values across the 0 mV to +40 mV range that reflect the assumption that heterozygous expression of L450F and G600R in the heart results in at least a 50% reduction in the observed I_{to} gain-of-function. The time constant of inactivation of the G600R mutant was increased by 19% in agreement with experimental data.

Statistical analysis

All data points represent the mean value and bars represent the standard error of the mean (SEM). Determination of statistical significance between two groups was accomplished using a Student *t*-test. One-way ANOVA was used among multiple group comparison. A *p* value of <0.05 was considered statistically significant.

Statement of Responsibility

The authors had full access to and take full responsibility for the integrity of the data. All authors have read and agree to the manuscript as written.

RESULTS

Mutation Analysis and Clinical Data

We molecularly interrogated *KCND3* in 86 unrelated genotype negative/phenotype positive patients with a referral diagnosis of Brugada syndrome that had been previously analyzed for mutations in the eight known BrS-susceptibility genes. Overall, 96% of patients were of Caucasian descent, 84% were male, the average age at diagnosis was 45±14 years, and 34% exhibited a spontaneous type I Brugada ECG pattern. Comprehensive mutational analysis of *KCND3* yielded two putative pathogenic mutations in two genetically elusive BrS cases.

Abnormal DHPLC elution profiles (Figure 1A) and subsequent direct DNA sequencing (Figure 1B) led to the identification of a *KCND3* c.348 C>T nucleotide substitution and a *KCND3* c.1798 G>C nucleotide substitution in two distinct genetically elusive BrS cases, which resulted in a L450F missense mutation (Lysine (L) for Phenylalanine (F) at position 450) and G600R missense mutation (Glycine [G] for Arginine [R] at position 600) respectively. Both the L450F and G600R missense mutations were absent from 1560 reference alleles ($p < 0.001$) and involve highly conserved residues located in the Kv4.3 carboxyl (C)-terminus (Figure 1C, 1D). The L450F- and G600R-positive BrS index cases were genotype-negative for mutations in the eight known BrS-susceptibility genes.

In addition, the analysis of *KCND3*'s seven translated exons in 780 ostensibly healthy controls revealed only 2 amino acid altering genetic variants (K214R and T486A), suggesting that *KCND3* harbors minimal background amino acid-altering genetic variation in comparison to other channelopathic genes.

The first BrS index case (Kv4.3-L450F) was a 45-year-old male with a history of heart palpitations at rest. No arrhythmias have been documented, but ST-segment elevation in leads V_1 and V_2 of the patient's resting Holter ECG were suspicious for BrS. There was no

documented history of syncope or cardiac events and the patient's family history was negative. He underwent a flecainide test that induced a type 1 ECG pattern (Figure 2A).

The second BrS index case (Kv4.3-G600R), a 22-year-old male with a history of heart palpitations and pre-syncope was discovered unconscious and unresponsive in bed. While hospitalized, a 12 lead ECG revealed ST-segment elevation in V_1, V_2, and V_3 and a QTc of 523 ms (data not shown). Cardiac enzymes were borderline normal with a creatine kinase of 370, a Troponin I of 0.32, and a relative index of 1.3. A complete cardiac work-up including echocardiogram and coronary angiogram were performed and found to be normal. All drug/toxicology screens were negative.

A follow-up ECG several days later revealed down sloping ST-segment elevation in the right precordial leads (V_1-V_3) with a normal PR-interval of 150 ms (Figure 2B). The patient's QT interval remained slightly prolonged. Given the patient's significant paternal family history of sudden cardiac death (paternal grandfather died suddenly at age 39 and a paternal uncle died suddenly at age 35) and the abnormal ECG findings suggestive of BrS, an internal cardiac defibrillator was implanted as a secondary prevention.

Heterologous Expression and Functional Characterization of Kv4.3-L450F and Kv4.3-G600R

In order to re-capitulate the I_{to} current *in vitro*, Kv4.3-WT, Kv4.3-L450F, or Kv4.3-G600R was heterologously co-expressed with KChIP2-WT in HEK293 cells (Figure 3A). Analysis of the current-voltage relationship indicated that Kv4.3-L450F or Kv4.3-G600R plus KChIP2-WT significantly increased I_{to} current density from 0 mV to +40 mV (n=15 for both mutations, $p<0.05$) compared with Kv4.3-WT plus KChIP2-WT (n=18, Figure 3B). Kv4.3-L450F and Kv4.3-G600R significantly increased current density at 0 mV by 154.3% and 48.1% percent respectively from 46.6±4.6 (WT, n=18) to 118.5±16.0 (L450F, n=15, $p<0.05$) and 69.0±10.6 (G600R, n=15, $p<0.05$) and similarly increased the peak current density at 40 mV by 146.2% and 50.4% respectively from 166.6±14.8 (WT, n=18) to 410.2±51.4 (L450F, n=15, $p<0.05$) and 250.5±34.2 (G600R, n=15, $p<0.05$, Figure 3C). Kv4.3-G600R plus KChIP2-WT exhibited significantly slower inactivation tau across the 0 mV to 40 mV range compared with Kv4.3-WT plus KChIP2-WT from 71.9±4.5 ms (WT at 40 mV, n=18) to 89.3±3.0 ms (G600R at 40 mV, n=15, $p<0.05$, Figure 4A). Kv4.3-L450F plus KChIP2-WT significantly increased I_{to} total charge by 117.0% at 40 mV (n=15, $p<0.05$) and Kv4.3-G600R plus KChIP2-WT significantly increased the I_{to} total charge by 58.3% at 40 mV (n=15, $p<0.05$) compared with Kv4.3-WT plus KChIP2-WT (n=18, Figure 4B).

Kv4.3-L450F significantly shifted $V_{1/2}$ of inactivation −5.2 mV from −21±0.7 mV (WT, n=12) to −26.2±0.7 mV (L450F, n=7, $p<0.05$, Figure 4C) while the Kv4.3-G600R mutation did not significantly alter the inactivation kinetics of I_{to} compared to Kv4.3-WT. The respective k (slope factor) remains unchanged for both mutations. The time constants for the recovery from inactivation, assessed using a two-pulse protocol (**see inset** Figure 4D **and figure legend**) were 57.4±1.7 ms for cells co-transfected with Kv4.3-WT plus KChIP2 (n=7), 55.2±1.6 ms for cells co-transfected with Kv4.3-L450F plus KChIP2 (n=5), and 61.6±1.8 ms for cells co-transfected with Kv4.3-G600R plus KChIP2 (n=6). There was no significant difference among the three groups.

Simulated Effect of Kv4.3-L450F and Kv4.3-G600R on the Right Ventricular Epicardial Action Potential

In order to simulate the experimentally observed effects of the L450F and G600R mutations on the RV action potential, a modified Luo-Rudy II AP model was utilized as previously

described.[16] Simulated I_{to} traces under standard voltage-clamp conditions during the step to 0 mV for 100 ms from a holding potential of −90 mV indicates that the heterozygous expression of Kv4.3-L450F or Kv4.3-G600R increases peak current by 72% and 25% respectively and that Kv4.3-G600R slows the inactivation time constant by 19.0% relative to WT (Figure 5A). These values closely recapitulate the properties expected to be associated with a 50% reduction of the experimentally obtained values for the Kv4.3-L450F and Kv4.3-G600R currents across the 0 mV to +40 mV range. The total charge carried by the simulated I_{to} current was increased 59% by L450F relative to WT and 29% by G600R relative to WT. This computer simulation was again similar to the experimentally observed values of 58.5% and 29.1% for L450F and G600R respectively that were derived from heterologous expression studies.

Simulated RV epicardial action potentials using Kv4.3-L450F, Kv4.3-G600R, and WT I_{to} currents were used to assess the ability of the L450F and G600R mutants to cause the loss of the AP dome in the modified Luo-Rudy II AP model. After several cycles of simulation at a basic cycle length (BCL) of 800 ms to allow for re-equilibration of intracellular Ca2+ concentrations, the simulated AP containing either Kv4.3-L450F or Kv4.3-G600R mutant I_{to} current yielded a marked and stable loss of the AP dome in comparison to Kv4.3-WT (Figure 5B).

DISCUSSION

The role of the I_{to} current remains central to “the repolarization disorder” theory of Brugada syndrome. The use of RV canine wedge preparations over the past decade has elucidated the critical role of the intrinsic I_{to}-mediated transmural voltage gradient in the inscription of the J wave under physiologic conditions[17] and the development of ST-segment elevation and reentrant ventricular arrhythmias in the presence of potassium channel activators[18] and sodium and calcium channel blockers[19] that function to amplify the intrinsic I_{to} gradient resulting in the loss of the action potential dome at some epicardial sites. Furthermore, the recording of monophasic action potentials of the RV outflow tract has demonstrated the presence of a prominent AP notch in the epicardium, but not the endocardium of patients with BrS providing clinical evidence that an I_{to}-mediated transmural gradient is present in humans.[20] Lastly, while sodium channel blockers have been shown to unmask or induce a type I BrS ECG pattern, the use of quinidine, a sodium channel blocker that also potently inhibits I_{to} has been demonstrated to normalize ST-segment elevation[21] in patients with BrS suggesting that the reduction of the I_{to} current may have clinical relevance.

Despite the growing body of evidence linking the I_{to} current to the pathogenesis of BrS, until recently there was minimal experimental data to directly implicate perturbations in I_{to} to disease. The identification of a BrS-associated loss-of-function missense mutation in *KCNE3* provided the first evidence that mutations resulting in an increase in I_{to} could produce a type I BrS ECG pattern.[10] Furthermore, canine wedge preparations treated with the I_{to}-specific activator NS5806 increased the I_{to}-mediated AP notch in epicardium, but not the endocardium leading to J wave accentuation, development of phase 2 reentry, and the initiation of ventricular tachycardia in both ventricles providing further evidence that I_{to} gain-of-function can recapitulate the hallmarks of BrS.[14]

Consistent with the established role of I_{to} in BrS pathogenesis, our present study demonstrates the first association of gain-of-function mutations in the *KCND3*-encoded Kv4.3 α-subunit that conducts I_{to} in humans with Brugada syndrome. Here, we present two unrelated cases, one an asymptomatic 45-year-old male with documented ST-segment elevation in the right precordial leads on Holter ECG and a positive flecainide test and the second, a 22-year-old male with a documented type I BrS ECG pattern, and a family history

of sudden death who was discovered unresponsive in bed. Both were found to harbor novel missense mutations in *KCND3*. In addition, these mutations involved highly conserved residues in the Kv4.3 C-terminus and were both absent in 1560 reference alleles.

The heterologous co-expression of both Kv4.3-L450F and Kv4.3-G600R with KChIP2 resulted in a gain-of-function in the I_{to} current. Further, simulations using a modified Luo-Rudy II AP model that incorporates an increase in I_{to} maximal conductance ($G_{Kv4.3}$) consistent with experimentally derived data (1.30 mS/μF, 1.56 mS/μF, and 2.32 mS/μF for WT, G600R, and L450F, respectively) demonstrated that the 73.1% increase in I_{to} current associated with Kv4.3-L450F and the modest 25.2% increase in I_{to} current together with a 19% slowing of I_{to} inactivation associated with Kv4.3-G600R are both capable of producing the stable loss of the AP dome in RV epicardial tissue.

Interestingly, simulations using the same modified Luo-Rudy II model that incorporates a smaller $G_{Kv4.3}$ intended to model the LV epicardial action potential (0.5 mS/μF and 0.7 mS/μF for WT and G600R respectively) did not demonstrate loss of the AP dome. The use of a smaller wild-type $G_{Kv4.3}$ (0.25 mS/μF) that fails to fully reproduce the deep right ventricular AP likely explains why a 3.5 fold acceleration of I_{Na} inactivation and a 7 fold increase in $G_{Kv4.3}$ (to 1.75 mS/μF) was required to simulate the ionic basis of BrS in a previous study that utilized a Luo-Rudy II AP model.[16] By setting wild-type I_{to} to a more physiologically relevant $G_{Kv4.3}$, the *in silico* modeling included in this study demonstrates that even the modest increase in I_{to} expected to be associated with the heterozygous expression of Kv4.3-G600R in the heart is capable of causing the loss of the AP dome in the RV epicardium.

While the role of the I_{to} current in producing the characteristic “spike and dome” morphology of the epicardial action potential is well established, the precise role of I_{to} in regulating the action potential duration (APD) in large mammals remains largely undefined. In both Winslow-Rice-Jafri canine ventricular cell and the Luo-Rudy II multi-cellular fiber AP models, the effect of increased Kv4.3 current density on canine AP shape and duration demonstrates a bimodal phenomenon, whereby increasing I_{to} current density in the presence of high baseline densities is predicted to shift the AP from a spike and dome morphology to a shortened AP that lacks the plateau phase.[22] Interestingly, in both models, increasing I_{to} current density in the presence of low baseline densities is predicted to result in a modest prolongation of the APD. Based on both single cell and multi-cellular AP modeling, the effect of I_{to} perturbations appears to be largely dependent on the strength of the underlying I_{to} current that the I_{to} alterations are superimposed on.

Thus, one could envision a scenario whereby the roughly 73.1% and 25.2% increase in I_{to} current density conferred by heterozygous expression of Kv4.3-L450F and Kv4.3-G600R in the heart might be expected to increase APD in the LV where I_{to} current density is relatively low, as was observed for Kv4.3-G600R (data not shown) and the I_{to} activator NS5806[14], resulting in a prolonged QT interval and the heterogeneous loss of the AP dome in RV epicardium were I_{to} current densities are the highest. While this scenario certainly fits with the clinical and electrophysiological phenotype associated with Kv4.3-L450F and Kv4.3-G600R, drawing a definitive conclusion on the impact of I_{to} gain-of-function mutations on the APD and thus QT interval based on existing modeling is complicated by the existing disagreement between various strand and single myocyte computational models in regards to the true role the I_{to} current plays in determining cardiac APD.[23]

Even though the exact effect of loss- and gain-of-function mutations in *KCND3* on the APD and QT interval in humans is not thoroughly understood, prolongation of the QT interval in the presence of ST-segment elevation appears to be a clinical hallmark in some BrS cases.[24] Thus, the presence of QT prolongation in G600R-positive BrS index case is consistent with

the clinical scenario of BrS and not necessarily an indication of an additional underlying channelopathy such as LQTS. The functional investigation of rare mutations in the *KCND3* may provide an important opportunity to deepen our understanding of the physiologic and pathophysiologic roles of the I_{to} current in shaping the human cardiac action potential.

Given the modest increase in I_{to} current associated with Kv4.3-L450F and Kv4.3-G600R we speculate that the gain-of-function mutations in *KCND3* may leave affected individuals susceptible to modest physiologic changes in the inward (I_{Na} and $I_{L,Ca}$) or outward (I_{to} and $I_{K\text{-}ATP}$) currents active during early repolarization. An increase in vagal tone during sleep or the activation of epicardial predominant IK-ATP currents as a result of metabolic stress could further exacerbate the genetically enhanced I_{to}-mediated transmural voltage gradient associated with Kv4.3-L450F or Kv4.3-G600R in the RV epicardium pushing the AP to more negative potentials resulting in the failure of the L-type calcium channel to activate and the heterogenous loss of AP dome at some epicardial sites.[9] Due to higher baseline levels of I_{to} expression in the right ventricular epicardium of males compared to females[25], males harboring I_{to} gain-of-function mutations are likely more sensitive to physiologic changes that can precipitate the arrhythmic manifestations of BrS than females, thus the identification of Kv4.3-L450F and Kv4.3-G600R in two male BrS index cases is therefore not surprising.

The discovery of rare BrS-associated I_{to} gain-of-function mutations in *KCND3* supports the hypothesis that a genetically enhanced transmural dispersion of repolarization in the RV may directly contribute to BrS pathogenesis. Given that loss-of-function mutations in Nav1.5-interacting proteins as well as the Cav1.2-interacting protein may contribute to ionic and electrocardiographic manifestations of BrS by exposing a large unopposed I_{to} current in the RV epicardium, it stands to reason that mutations in genes encoding Kv4.3-interacting proteins or genetic regulators of *KCND3* expression that enhance the I_{to}-mediated transmural voltage gradient could function as novel pathogenic substrates for BrS. Further interrogation of the Kv4.3 macromolecular complex and regulators of *KCND3* expression is needed to elucidate the role of the I_{to} current in the pathogenesis of BrS and other J-wave syndromes.

Conclusion

In conclusion, this study provides the molecular and functional evidence necessary to implicate *KCND3* as a novel BrS-susceptibility gene (KCND3-BrS or BrS9). Further studies are warranted to fully elucidate the mechanisms responsible for the increase in I_{to} current observed with Kv4.3-L450F and Kv4.3-G600R and the full extent to which rare I_{to} gain-of-function mutations contribute to BrS pathogenesis.

Acknowledgments

We acknowledge support for this work from the Mayo Clinic Windland Smith Rice Comprehensive Sudden Cardiac Death Program (M.J.A.), the Dr. Scholl Foundation (R.M.A., M.J.A.), the Hannah Wernke Memorial Foundation (M.J.A.), and the National Institutes of Health (R01-HD42569 to M.J.A., R01-HL47678 to C.A. and F30-HL106993 to J.R.G).

Abbreviations

AP	action potential
APD	action potential duration
BrS	Brugada Syndrome

I_{to}	transient outward current
DHPLC	denaturing high performance liquid chromatography
ECG	electrocardiogram
$G_{Kv4.3}$	I_{to}/Kv4.3 maximal conductance
Kv4.3	voltage-gated potassium channel
LQTS	Long QT Syndrome
LV	left ventricle
PCR	polymerase chain reaction
RV	right ventricle
SCD	sudden cardiac death

REFERENCES

1. Zheng ZJ, Croft JB, Giles WH, Mensah GA. Sudden cardiac death in the United States, 1989 to 1998. Circulation. 2001 Oct 30.104:2158–2163. [PubMed: 11684624]
2. Ellsworth EG, Ackerman MJ. The changing face of sudden cardiac death in the young. Heart Rhythm. 2005 Dec.2:1283–1285. [PubMed: 16360078]
3. Wren C. Sudden death in children and adolescents. Heart. 2002 Oct.88:426–431. [PubMed: 12231612]
4. Liberthson RR. Sudden death from cardiac causes in children and young adults. N Engl J Med. 1996 Apr 18.334:1039–1044. [PubMed: 8598843]
5. Tester DJ, Ackerman MJ. Postmortem long QT syndrome genetic testing for sudden unexplained death in the young. J Am Coll Cardiol. 2007 Jan 16.49:240–246. [PubMed: 17222736]
6. Antzelevitch C, Brugada P, Borggrefe M, et al. Brugada syndrome: report of the second consensus conference: endorsed by the Heart Rhythm Society and the European Heart Rhythm Association. Circulation. 2005 Feb 8.111:659–670. [PubMed: 15655131]
7. Chen PS, Priori SG. The Brugada syndrome. J Am Coll Cardiol. 2008 Mar 25.51:1176–1180. [PubMed: 18355655]
8. Kapplinger JD, Tester DJ, Alders M, et al. An international compendium of mutations in the SCN5A-encoded cardiac sodium channel in patients referred for Brugada syndrome genetic testing. Heart Rhythm. 2010 Jan.7:33–46. [PubMed: 20129283]
9. Antzelevitch C, Yan GX. J wave syndromes. Heart Rhythm. 2010 Apr.7:549–558. [PubMed: 20153265]
10. Delpon E, Cordeiro JM, Nunez L, et al. Functional effects of KCNE3 mutation and its role in the development of Brugada syndrome. Circ Arrhythm Electrophysiol. 2008 Aug.1:209–218. [PubMed: 19122847]
11. Medeiros-Domingo A, Tan BH, Crotti L, et al. Gain-of-function mutation S422L in the KCNJ8-encoded cardiac K(ATP) channel Kir6.1 as a pathogenic substrate for J-wave syndromes. Heart Rhythm. 2010 Oct.7:1466–1471. [PubMed: 20558321]
12. Ackerman MJ, Tester DJ, Jones GS, Will ML, Burrow CR, Curran ME. Ethnic differences in cardiac potassium channel variants: implications for genetic susceptibility to sudden cardiac death and genetic testing for congenital long QT syndrome. Mayo Clin Proc. 2003 Dec.78:1479–1487. [PubMed: 14661677]
13. Rozen S, Skaletsky H. Primer3 on the WWW for general users and for biologist programmers. Methods Mol Biol. 2000; 132:365–386. [PubMed: 10547847]
14. Calloe K, Cordeiro JM, Di Diego JM, et al. A transient outward potassium current activator recapitulates the electrocardiographic manifestations of Brugada syndrome. Cardiovasc Res. 2009 Mar 1.81:686–694. [PubMed: 19073629]

15. Dumaine R, Towbin JA, Brugada P, et al. Ionic mechanisms responsible for the electrocardiographic phenotype of the Brugada syndrome are temperature dependent. Circ Res. 1999 Oct 29.85:803–809.. [PubMed: 10532948]

16. Gima K, Rudy Y. Ionic current basis of electrocardiographic waveforms: a model study. Circ Res. 2002 May 3.90:889–896. [PubMed: 11988490]

17. Yan GX, Antzelevitch C. Cellular basis for the electrocardiographic J wave. Circulation. 1996 Jan 15.93:372–379. [PubMed: 8548912]

18. Yan GX, Antzelevitch C. Cellular basis for the Brugada syndrome and other mechanisms of arrhythmogenesis associated with ST-segment elevation. Circulation. 1999 Oct 12.100:1660–1666. [PubMed: 10517739]

19. Fish JM, Antzelevitch C. Role of sodium and calcium channel block in unmasking the Brugada syndrome. Heart Rhythm. 2004 Jul.1:210–217. [PubMed: 15851155]

20. Kurita T, Shimizu W, Inagaki M, et al. The electrophysiologic mechanism of ST-segment elevation in Brugada syndrome. J Am Coll Cardiol. 2002 Jul 17.40:330–334. [PubMed: 12106940]

21. Hermida JS, Denjoy I, Clerc J, et al. Hydroquinidine therapy in Brugada syndrome. J Am Coll Cardiol. 2004 May 19.43:1853–1860. [PubMed: 15145111]

22. Greenstein JL, Wu R, Po S, Tomaselli GF, Winslow RL. Role of the calcium-independent transient outward current I(to1) in shaping action potential morphology and duration. Circ Res. 2000 Nov 24.87:1026–1033. [PubMed: 11090548]

23. Decker KF, Heijman J, Silva JR, Hund TJ, Rudy Y. Properties and ionic mechanisms of action potential adaptation, restitution, and accommodation in canine epicardium. Am J Physiol Heart Circ Physiol. 2009 Apr.296:H1017–1026. [PubMed: 19168720]

24. Pitzalis MV, Anaclerio M, Iacoviello M, et al. QT-interval prolongation in right precordial leads: an additional electrocardiographic hallmark of Brugada syndrome. J Am Coll Cardiol. 2003 Nov 5.42:1632–1637. [PubMed: 14607451]

25. Di Diego JM, Cordeiro JM, Goodrow RJ, et al. Ionic and cellular basis for the predominance of the Brugada syndrome phenotype in males. Circulation. 2002 Oct 8.106:2004–2011. [PubMed: 12370227]

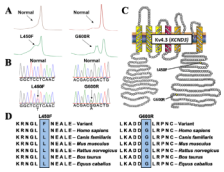

Figure 1. Identification of KCND3-L450F and KCND3-G600R Mutations in BrS

Mutations in *KCND3* are associated with Brugada syndrome. Depicted are A, DHPLC profiles (normal, red trace and abnormal, green trace) and B, DNA sequencing chromatograms. C, Predicted protein topology schematic of Kv4.3 indicating the location of the L450F and G600R mutations. D, Sequence conservation across species for the L450F and G600R mutations.

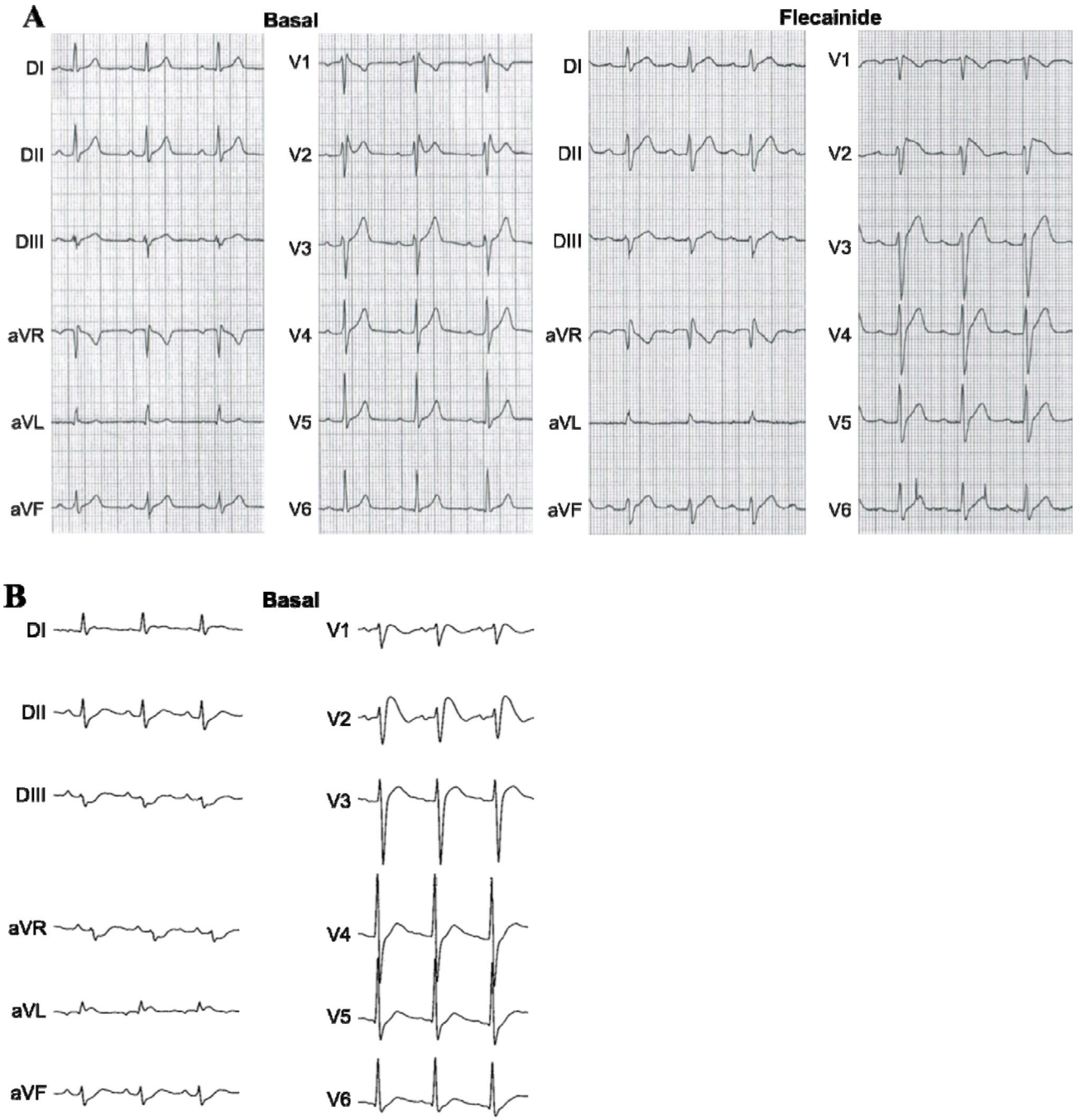

Figure 2. Representative Electrocardiograms for the L450F- and G600R-Positive BrS Index Cases

A, Representative basal Holter ECG demonstrating spontaneous ST-segment elevation in leads V_2 and V_3 and flecainide challenge twelve-lead ECG which unmasked a coved-type BrS ECG pattern in the L450F-positive BrS index case.

B, Representative baseline twelve-lead ECG of the G600R-positive BrS index case with V_1 through V_3 leads in the normal position.

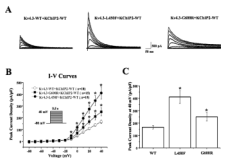

Figure 3. Kv4.3-L450F and Kv4.3-G600R Plus KChIP2 Increase I_{to} Current in Heterologous Cells

A, Representative whole-cell Kv4.3-WT plus KChIP2-WT (left), Kv4.3-L450F plus KChIP2-WT (middle) and Kv4.3-G600R plus KChIP2-WT (right) traces recorded in HEK293 cells elicited by step depolarization of 500 ms duration to +40 mV from a holding potential of −80 mV in 10 mV increments.

B, The current voltage relationship for WT (n= 18), L450F (n=15) and G600R (n=15) Kv4.3 channels co-expressed with KChIP2-WT. All values represent mean±SEM. * $p<0.05$ vs. Kv4.3-WT plus KChIP2-WT.

C. Bar graph showing peak current density at 40 mV for WT (n= 18), L450F (n=15) and G600R (n=15) Kv4.3 channels co-expressed with KChIP2-WT. * $p<0.05$ vs. Kv4.3-WT plus KChIP2-WT.

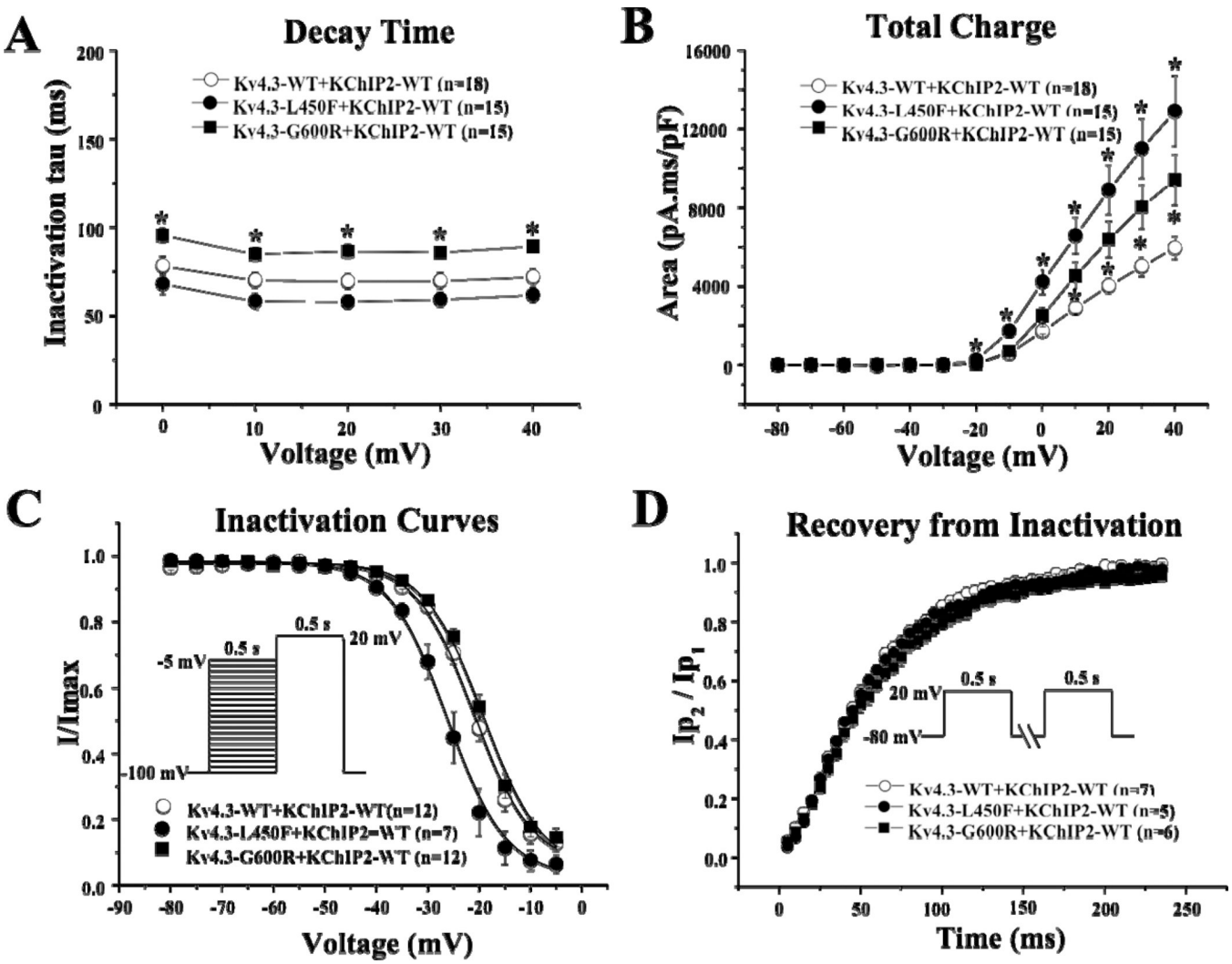

Figure 4. Kinetic Alteration for Kv4.3-WT, Kv4.3-L450F, or Kv4.3-G600R plus KChIP2

A, Inactivation time constants (τ) for Kv4.3-WT, Kv4.3–L450F, or Kv4.3–G600R plus KChIP2 currents plotted as a function of voltage. Inactivation time constants for each voltage step were determined by fitting a monoexponential function to current decay. All values represent mean±SEM. * $p<0.05$ vs. Kv4.3-WT plus KChIP2.

B, Total charge of Kv4.3-WT, Kv4.3-L450F, or Kv4.3–G600R with KChIP2 as a function of voltage obtained by measuring the area under curve during the first 50 ms of each voltage step. * $p<0.05$ vs. Kv4.3-WT plus KChIP2.

C, Steady-state inactivation curves of Kv4.3-WT, Kv4.3-L450F, or Kv4.3–G600R with KChIP2 determined from a holding potential of −100 mV to pre-pulse of −5 mV in 5 mV increments with 0.5 s duration followed by a test pulse of +20 mV with 0.5 s duration and fitted with a Boltzmann function.

D, Recovery from inactivation of Kv4.3-WT, Kv4.3-L450F, or Kv4.3-G600R with KChIP2 determined from a holding potential of −80 mV to pre-pulse of +20 mV with 0.5s duration, with increased recovery interval, followed by a test pulse of +20 mV with 500 ms duration and fitted with a one-exponential function. All values shown represent Mean ±SEM.

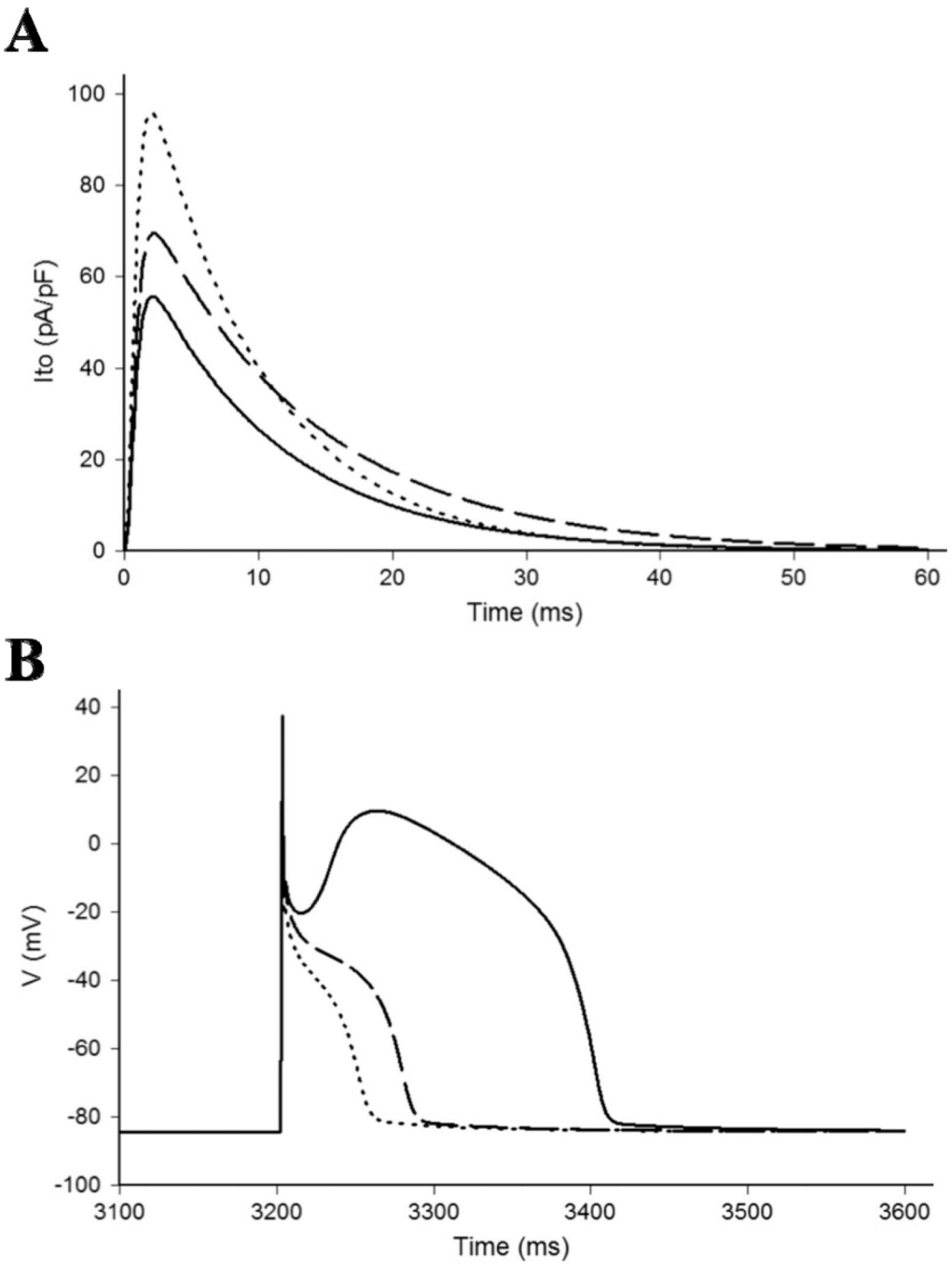

Figure 5. Effects of Kv4.3-L450F and Kv4.3-G600R on the Right Ventricular Epicardial Action Potential

A, Simulated I_{to} current traces during step depolarization for 100 ms to 0 mV from a holding potential of −90 mV. Only first 60 ms are shown. Solid line – WT; dotted line – L450F; dashed line – G600R.

B, RV epicardial action potentials simulated using WT, L450F, and G600R mutant I_{to} incorporated into a modified Luo-Rudy II AP model. BCL = 800 ms (75 bpm). Solid line – WT; dotted line – L450F; dashed line – G600R. Only the 5th AP in the equilibration chain is displayed here, the AP shape does not change in subsequent cycles.